Jamming and geometric representations of graphs

Werner Krauth[1] and Martin Loebl[2]

[1]CNRS-Laboratoire de Physique Statistique
Ecole Normale Supérieure, Paris
werner.krauth@ens.fr

[2]Department of Applied Mathematics and Institute for Theoretical Computer Science
Charles University, Prague
loebl@kam.mff.cuni.cz

Submitted: Apr 29, 2005; Accepted: Jun 27, 2006; Published: Jul 11, 2006
Mathematics Subject Classifications: 05C62, 05C70

Abstract

We expose a relationship between jamming and a generalization of Tutte's barycentric embedding. This provides a basis for the systematic treatment of jamming and maximal packing problems on two-dimensional surfaces.

1 Introduction

In a seminal paper [1], W. T. Tutte addressed the problem of how to embed a three-connected planar graph in the plane. He proposed to fix the positions of the vertices of one face (outer vertices) as the vertices of a convex n–gon and to let the other (inner) vertices of the graph to be positioned into the barycenters of their neighbors (see Fig. 1).

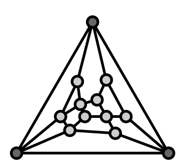

Figure 1: Barycentric embedding of a graph with $N = 13$ vertices (three outer vertices).

The barycentric embedding is unique. If we denote by $\mathbf{r}_1, \ldots, \mathbf{r}_N$ the positions of vertices of a graph with N vertices then the barycentric embedding minimizes the energy

$$E = \sum_{\text{edges } (i,j)} |\mathbf{r}_i - \mathbf{r}_j|^2$$

(proportional to the mean squared edge length) over the positions of the inner vertices (see [1]).

The purpose of this paper is to study *jamming*, a problem of importance for the physics of granular materials and of glasses [2, 3, 4], which also has many applications in mathematics and computer science [5]. We expose a relationship between jamming and a generalization of the barycentric embedding, and provide a basis for the systematic treatment of jamming on two-dimensional surfaces. We first informally describe our results and leave the formal definitions to the following sections.

A set of non-overlapping disks of equal radius may contain a sub-set of disks which do not allow any small moves, regardless of the positions of the other disks: In Fig. 2 (showing disks in a square), disks i,j,k,l,m, and n are jammed, while o is free to move.

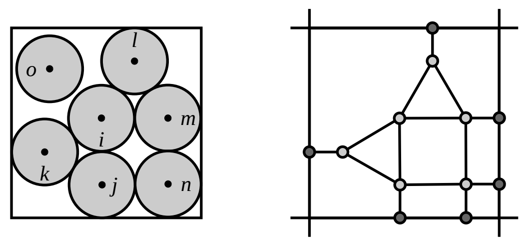

Figure 2: *Left:* Configuration of seven disks in a square. Disks i,j,k,l,m, and n are jammed. *Right:* Contact graph of the jammed sub-set. Edges among outer vertices are omitted.

The position $\mathbf{r}_i$ of the center of disk i must be at least a disk diameter away from other disk centers, and at least a disk radius from the boundary. If disk i is jammed, $\mathbf{r}_i$ locally maximizes the minimum distances to all other disks, and twice the distances to the boundaries. Hence for a disk i not in contact with the boundary, we have

$$\min_{j \neq i} |\mathbf{r}_i - \mathbf{r}_j| = loc \ \max_{\mathbf{r}} \min_{j \neq i} |\mathbf{r} - \mathbf{r}_j|,$$

where loc means that $\mathbf{r}_i$ is in a local maximum. In the past, many authors [6] have found excellent jammed configurations of disks on a sphere by searching for local minima of the repulsive energy

$$E(\mathbf{r}) = \sum_{j \neq i} |\mathbf{r} - \mathbf{r}_j|^{-q} \tag{1}$$

in the limit $q \to \infty$ where, evidently, the small distances $|\mathbf{r} - \mathbf{r}_j|$ contribute most, so that the local minima of the energy become equivalent to hard-disk configurations. As the minimum is local, one cannot prove that with this method the best jammed configuration is generated.

The relationship between jamming and the geometric representation of graphs was first pointed out, a long time ago, by Schütte and van der Waerden [7]. Each center of a jammed disk corresponds to an inner vertex of a graph, and each touching point with the boundary to an outer vertex. The edges of the graph refer to contact of disks among themselves and with the boundary, as shown in Fig. 2. Such an embedded graph uniquely determines the configuration of disks. The key problem is to find a crucial necessary property of the graphs corresponding to the jammed configurations, which allows a successful mathematical treatment.

In this paper, we propose and investigate the property that, in the example of Fig. 2, each position $\mathbf{r}_i$ is not only the local maximum of the minimum distance to all other disks, but also the *global* minimum of the maximum length of the edges involving vertex i

$$\max_{a=j,k,l,m} |\mathbf{r}_i - \mathbf{r}_a| = \min_{\mathbf{r}} \max_{a=j,k,l,m} |\mathbf{r} - \mathbf{r}_a|. \tag{2}$$

For an arrangement of disks, as in Fig. 2, it is trivial that the position $\mathbf{r}_i$ realizes this minimum. In this paper, we study special representations of graphs that we call $\mathcal{M}$–representations (as in Fig. 2), with inner vertices (the ones drawn in light gray, in Fig. 2) and possibly outer vertices (in dark gray). These graphs are defined without reference to disk packings, but only through the property that each vertex minimizes the maximum (rescaled) distance to its neighbors (as in eq. (2)). This makes the notion of the $\mathcal{M}$–representation non-trivial. It generalizes Tutte's barycentric embedding where each edge realizes the minimum of the mean squared distance, as discussed before. Outer vertices are either fixed or restricted to line segments (see section 2 for precise definition).

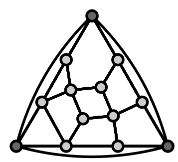

Figure 3: Stable $\mathcal{M}$–representation of the graph of Fig. 1, with identical positions of the outer vertices. Three faces of this representation are flat.

We define *stable* representations as $\mathcal{M}$–representations which are local minima with respect to an ordering relation. This relation replaces the notion of an energy which cannot be defined in this setting.

We establish that the stable representation in the plane, torus, or on the hemisphere is essentially unique for any graph. We show that $\mathcal{M}$–representations of three-connected planar and toroidal graphs are convex pseudo-embeddings, and that the set of regular three-connected stable representations contains all jammed configurations. This puts jamming in direct analogy with the barycentric embeddings. On the sphere, stable representations are not unique, but we conjecture that their structure is restricted.

One application of jamming is the generation of packings of N non-overlapping disks with maximum radius. Such a maximal packing contains a non-trivial jammed sub-set, since otherwise we could increase the radius of each disk. The remaining disks of a maximal packing are not jammed (as disk o in Fig. 2), and confined to holes in the jammed sub-set. In these holes, we can again search for jammed configurations with suitably rescaled radii. This gives a recursive procedure to compute maximal disk packings, which relies on the enumeration of (three–connected) planar or toroidal graphs and a computation of their jammed representations which form a sub-set of the stable representations. Practically, we generate the stable representation with a variant of the minover algorithm [8] which appears to always converge to a stable solution, on the plane, torus, and on the sphere.

The most notorious instance of maximal packing is the $N = 13$ spheres problem for disks on the sphere. It has been known since the work of Schütte and van der Waerden [7] that 13 unit spheres cannot be packed onto the surface of the unit central sphere (a popular description has appeared recently in the French edition of Scientific American [9]). However, the minimum radius of the central sphere admitting such a packing is still unknown, as it is for all larger N, with the exception of $N = 24$ [10]. The problem of packing spheres on a central sphere is clearly equivalent to the problem of packing disks on a sphere.

Our strategy for solving the maximal packing problem will be complete once the following conjectures are validated:

Conjecture 1. *There exists a finite algorithm to find a stable representation of a given graph.*

Conjecture 2. *Each graph on the sphere with a fixed set of edges crossing a given equator has at most one non-trivial stable representation up to symmetry transformations on the sphere. Furthermore, jammed configurations are stable.*

At present, we are able to prove Conjecture 2 for a fixed *representation* of edges across an equator, rather than their set. The conjecture is backed by extensive computational experiments. For planar region and torus, only Conjecture 1 is needed.

2 $\mathcal{M}$–representations

In this section we discuss representations of graphs in a planar region, on the torus, and the sphere. By *torus* we mean a rectangular planar region where the parallel sides are formally identified. In a representation, each vertex is a point, and each edge the shortest connection between vertices. It is possible for several, or all the points to coincide. Some or all of the edges then have zero length.

A shortest connection between two points will be also called line segment.

Definition 1 (Inner and outer vertices). *We assume that a possibly empty subset $\mathcal{O}$ of vertices (we will call them* outer*) is specified in each graph. Each representation of an outer vertex is fixed or constrained to lie on a specified line segment. Moreover we require that these restrictions of the positions of the outer vertices are such that any allowed choice of the outer vertices positions forms a subdivision of a convex n-gon.*

An edge between an inner and an outer vertex is represented by the shortest connection from the inner vertex to the feasible region of the outer vertex. A position of a vertex i in a representation will be denoted by $\mathbf{r}_i$.

The intuition behind the outer vertices is that the inner vertices belong to the convex hull of the outer vertices. This is indeed the case in all the situations considered in the paper (each time it follows from the particular circumstances).

On the torus, the rectangle can always be chosen so that vertices do not lie on its sides. We require that in a representation the shortest connection between vertices connected by an edge is uniquely determined. A representation is an *embedding* if it corresponds to a proper drawing, i.e. the representations of the vertices are all different and the interiors of the representations of the edges are disjoint and do not contain a representation of a vertex. We recall that a graph is k-connected if it has more than k vertices and remains connected after deletion of any subset of $k-1$ vertices. Furthermore, we use two basic facts of graph-theory: the faces of a two-connected planar embedding are bounded by cycles, and embeddings of a three-connected planar graph have a unique list of faces and incidence relations.

Each toroidal representation of a graph gives rise to a unique periodic representation by tiling the plane with the rectangles, as shown in Fig. 4. A *proper* toroidal representation has edges crossing each side of the rectangle and no outer vertices.

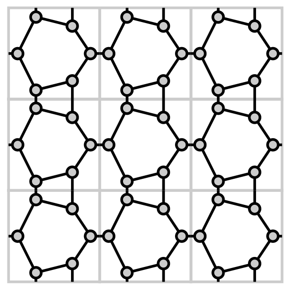

Figure 4: The periodic representation of a toroidal graph with six vertices.

As indicated in the introduction, we define a rescaled distance, in order to treat outer and inner vertices on the same footing.

Definition 2 (Rescaled distance). *The distance between vertices i and j is*

$$\gamma_{ij}|\mathbf{r}_i - \mathbf{r}_j|,$$

where $\gamma_{ij} = 1$ if both i, j are inner vertices, and $\gamma_{ij} = d \geq 1$ if one of the vertices is inner and the other one outer. The distance between two outer vertices is irrelevant ($| \quad |$ denotes the Euclidean distance). In a given representation, we denote by $l(e)$ the (rescaled) length of an edge e, i.e. the distance between its end-vertices.

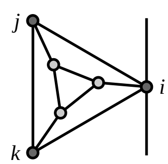

Figure 5: Representation of planar graph in the plane. The outer vertex i is constrained to lie on a line segment, whereas j and k are fixed.

2.1 $\mathcal{M}$–center of vectors

Let $\mathbf{r}_i,\ i \in I$ be a finite collection of vectors. The *radius* ρ of a vector $\mathbf{r}$ w.r.t. this collection is defined by $\rho(\mathbf{r}) = \max_i |\mathbf{r} - \mathbf{r}_i|_\gamma$.

Definition 3 (Radius). *The $\mathcal{M}$–center of a finite number of vectors $\mathbf{r}_i,\ i \in I$ is the vector $\mathbf{r}_\infty$ minimizing the radius w.r.t. this collection:*

$$\rho(\mathbf{r}_\infty) = \min_{\mathbf{r}}\ \rho(\mathbf{r}).$$

The $\mathcal{M}$–center is locally unique: If there were two close $\mathcal{M}$–centers with the same radius ρ, then the intersection of the corresponding circles of radius ρ would contain all the neighbors, but this intersection is contained in a circle of smaller radius.

Lemma 1 (No local minimum besides global one). *If $\mathbf{r}$ is not the $\mathcal{M}$–center of vectors $\mathbf{r}_i,\ i \in I$, then for each $\delta > 0$ there is a vector $\mathbf{r}'$ with $|\mathbf{r}' - \mathbf{r}| < \delta$ such that $\rho(\mathbf{r}) > \rho(\mathbf{r}')$.*

We note that the $\mathcal{M}$–center of vectors $\mathbf{r}_i,\ i \in I$, is the center of a circle touching more than one point. If it touches only two points, the circle must be in the center of them. On the other hand, if it passes through three points, these points define the center uniquely. To determine it, we construct, for each pair and also for each triple of vectors, this unique circle. The center of the smallest circle with no point on its outside is the $\mathcal{M}$–center.

Definition 4 ($\mathcal{M}$–representation). *An $\mathcal{M}$–representation of a graph is a representation where each inner vertex is the $\mathcal{M}$–center of its neighbors.*

Definition 5 (Pseudo–embedding). *A representation of a graph in the plane or a hemisphere is called a* pseudo–embedding *if it is an embedding except that some faces may collapse into a line segment. Such faces will be called* flat*. Moreover, a* convex pseudo–embedding *has convex faces and each flat face is a topological subdivision of C_2, a cycle of length two.*

An example of a convex pseudo–embedding is shown in Fig. 3.

The following proposition is proven in a sequence of ten lemmas.

Proposition 1. *Let $\mathcal{E}$ be a representation of a three-connected planar graph on a plane or hemisphere, such that each inner vertex belongs to the convex hull of its neighbors, with non-empty set of outer vertices. Then $\mathcal{E}$ is a convex pseudo–embedding.*

Proof. We proceed analogously to the paragraphs 6-9 of [1]. Since G is three-connected, its set of faces is uniquely determined, and each face is bounded by a cycle. $\mathcal{O}$ denotes the set of outer vertices.

Let l be a line in the plane or a non-trivial intersection of a plane with the hemisphere and define $g(v), v \in V$, as the perpendicular distance of v to l, counted positive on one side and negative on the other side of l.

The outer vertices with the greatest value of g are called *positive poles* and those with the least value of g are *negative poles*. The sets of positive and negative poles are disjoint since $\mathcal{O}$ is non-empty and hence the positions of the vertices of $\mathcal{O}$ form a subdivision of a convex n–gon.

A simple path $P = v_1, \ldots, v_k$ of G is *right (left) rising* if for each i, $g(v_i) < g(v_{i+1})$ or $g(v_i) = g(v_{i+1})$ and v_{i+1} is on the right (left) hand-side of v_i with respect to l (this is not difficult to formalize e.g. by fixing an orientation of l. Right (left) falling paths are defined analogously.

Lemma 2. *Each vertex v of G different from a pole has two neighbors v' and v'' so that $g(v') < g(v) < g(v'')$ or $g(v') = g(v) = g(v'')$ and v belongs to the line between v' and v''.*

Proof. This follows for outer vertices since they form a subdivision of a convex n–gon, and for inner vertices because of the convexity assumption. ☐

Lemma 3. *Let v be a vertex of G. There is a right rising and a left rising path from v to a positive pole, and also both right and left falling paths from v to a negative pole.*

Proof. By Lemma 2 v has a neighbor v' with $g(v') > g(v)$ or $g(v') = g(v)$ and v' is on the right hand-side of v. Since G is three-connected, v' has a neighbor different from v. Using Lemma 2, we can monotonically continue from v'. This constructs a right rising path, and the remaining paths may be obtained analogously. ☐

Lemma 4. *If $v \notin \mathcal{O}$ then v belongs to the convex hull of $\mathcal{O}$.*

Proof. If such v does not belong to the convex hull of $\mathcal{O}$, then let l be a line in the plane (cycle on the hemisphere) which defines a separating plane, and we get a contradiction with Lemma 3. ☐

Lemma 5. *Let F be a face of G and v_1, v_1', v_2, v_2' vertices of F appearing along F in this order. Then G does not have two disjoint v_1, v_2 and v_1', v_2' paths.*

Proof. This is a simple property of a face of a planar graph. ☐

Lemma 6. *If a face F is flat then it is a topological subdivision of C_2. Furthermore, let e be an edge of a face F and let l be a line in the plane (a cycle on the hemisphere) containing e. Then F is embedded on one side of l.*

Proof. This simply follows from Lemma 3 and Lemma 5 (see Fig. 6). ☐

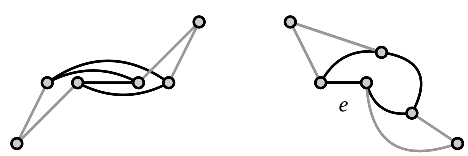

Figure 6: *Left:* a flat face must be a subdivision of C_2. *Right:* each face must lie on one side of incident edge e.

It follows from Lemma 6 that each face is a subdivision of a convex n–gon or flat and subdivision of C_2.

Each edge belongs to exactly two different faces. An edge is *redundant* if it belongs to two flat faces. More generally, in a two-connected representation with prescribed faces such that each flat face is a subdivision of C_2, a path which is a subdivision of an edge is *r*edundant if it belongs to two flat faces. A graph is a *simplification* of G if some redundant edges and, thereafter, maximal redundant paths have been deleted.

Lemma 7. *A flat face of a simplification of G is a subdivision of C_2.*

Proof. If we delete e and unify the two faces containing e, we get a planar graph. If the statement does not hold then we can again use Lemma 3 and Lemma 5 to obtain a contradiction. The same applies for a maximal redundant path. ☐

Let G' be the smallest simplification of G and let F be a flat face of G'. We know that it is a subdivision of C_2, and each edge of F belongs to one of the two sides of C_2.

Lemma 8. *Let e be an edge of G' and let l be the line in the plane (cycle on the hemisphere) containing e.*

1. *If e belongs to a flat face F, then the faces incident with edges of different sides of F are on opposite sides of l.*

2. *If edge e does not belong to a flat face, then the two faces incident with e lie on opposite sides of l.*

Proof. For the second property: as in the proof of Lemma 7, if we delete e and 'unify' the two faces containing e, we get a planar graph. If the two faces lie on the same side of e, we can use Lemma 5. The first property is analogous. ☐

Let $|G|$ denote the subset of the surface consisting of the embeddings of the vertices and edges of G, and let S denote the complement of $|G|$.

We define a function d on S as follows: $d(x) = 1$ if x is not within the convex hull of $\mathcal{O}$, otherwise, $d(x)$ equals the number of interiors of faces to which x belongs. The correctness of this definition is guaranteed by Lemma 4.

Lemma 9. *For each $x \in S$, $d(x) = 1$.*

Proof. It follows from Lemma 8 that the function d does not change when passing an edge. However, it cannot change elsewhere and outside of the convex hull of $\mathcal{O}$ it equals to 1. Hence it is 1 everywhere. ☐

Lemma 10. *If an edge e intersects the interior of an edge e', then one of them is not in G' or they belong to opposite sides of a flat face of G'.*

Proof. This is a corollary of Lemma 9. ☐

☐

The notion of the pseudo–embedding may be extended to the representations of a graph on the sphere and to the proper toroidal representations. Here we say that a face is convex if it contains a shortest connection between any pair of its points.

Corollary 1 ($\mathcal{M}$–rep. is pseudo–embedding). *An $\mathcal{M}$–representation without outer vertices of three-connected planar graphs on a sphere or three-connected proper toroidal graphs on a torus is a convex pseudo–embedding.*

Proof. As the number of vertices is finite, we can always find a cut (rectangle and plane through the center, respectively), which does not contain any intersection of two edges. The corollary follows by taking as outer vertices the intersection of edges with the cut. If the cut does not intersect any edges, the representation is trivial. □

Definition 6 (Ordering of representations). *Consider two representations $\mathcal{E}$ and $\mathcal{E}'$ of a graph G. We say that $\mathcal{E}$ is* smaller *than $\mathcal{E}'$ ($\mathcal{E} < \mathcal{E}'$) if the ordered vector of lengths of the edges containing an inner vertex of $\mathcal{E}$ is lexicographically smaller than the ordered vector of lengths of the same edges in $\mathcal{E}'$.*

The above ordering relation cannot generally be mapped into the real numbers, because the real axis does not admit an uncountable number of disjoint intervals. Therefore, there is no 'energy' (generalizing eq. (1)) such that $\mathcal{E} < \mathcal{E}' \Leftrightarrow E(\mathcal{E}) < E(\mathcal{E}')$.

Definition 7 (Stable representation). *Consider a representation $\mathcal{E}$ of a graph $G = (V, E)$ with inner, and possibly outer vertices i at positions $\mathbf{r}_i$. $\mathcal{E}$ is* stable *if there exists a value δ such that all embeddings $\mathcal{E}'$ of G with vertices at $\mathbf{r}'_i$ with $|\mathbf{r}_i - \mathbf{r}'_i| < \delta \ \forall i$ satisfy $\mathcal{E}' \geq \mathcal{E}$.*

Proposition 2. *Stable representations are $\mathcal{M}$–representations.*

Proof. Let the vertex i of $\mathcal{E}$ have the radius ρ_i and let edge $\{i, j\}$ have length ρ_i. Note that $\rho_j \geq \rho_i$. If i is not the $\mathcal{M}$–center of its neighbors, then it follows from Lemma 1 that there is a representation $\mathcal{E}'$ obtained from $\mathcal{E}$ by a small move of vertex i, such that $\rho'_i < \rho_i$. All edges $\{k, l\}$ with length bigger than ρ_i are the same in $\mathcal{E}$ and $\mathcal{E}'$. No edge $\{k, l\}$ of length ρ_i in $\mathcal{E}$ is longer in $\mathcal{E}'$ and at least one such edge has shortened. Finally, edges $\{k, l\}$ shorter than ρ_i in $\mathcal{E}$ may become longer in $\mathcal{E}'$. As a result, we have $\mathcal{E}' < \mathcal{E}$, which is impossible for a stable representation. □

Proposition 3 (Existence of stable representation). *Each graph has a stable representation.*

Proof. Let $\delta > 0$ be a sufficiently small constant. Define a sequence of representations $\mathcal{E}_1, \mathcal{E}_2, \ldots$ as follows: $\mathcal{E}_1$ is arbitrary. If $\mathcal{E}_i$ is unstable let $\mathcal{E}_{i+1}$ be a lexicographically minimal representation where each vertex has moved by at most δ (it exists by compactness). In particular $\mathcal{E}_{i+1} < \mathcal{E}_i$. Again by compactness, there is a converging subsequence of representations $\mathcal{E}'_j$ with limit $\mathcal{E}'$. $\mathcal{E}'$ must be stable since otherwise for $\mathcal{E}'_i$ very near to $\mathcal{E}'$, there is a close-by representation $\overline{\mathcal{E}} < \mathcal{E}'$. Taking into account the minimality rule in the construction of the sequence of representations, this contradicts the assumption that $\mathcal{E}'_i$ monotonically decreases in lexicographic order to $\mathcal{E}'$. □

Note that the stable representation can consist in all vertices falling onto a single point. This stable representation is unique for a graph without outer vertices in a plane or on the hypersphere. This stable representation also exists, but is usually not unique, for a graph without outer vertices on the sphere.

2.2 Uniqueness of stable representations

Proposition 1 implies that each $\mathcal{M}$–representation is a convex pseudo–embedding. Whereas Tutte's barycentric embedding is unique, the $\mathcal{M}$–representations are not necessarily unique, as can be seen by the counter-example sketched in Fig. 5 (the vertices of the inner triangle are in $\mathcal{M}$–position; they can be rotated and rescaled, to remain in $\mathcal{M}$–position). However, there is a unique *stable* representation.

Lemma 11. *Consider two-dimensional vectors* $\mathbf{r}_1, \mathbf{r}_2, \mathbf{r}'_1, \mathbf{r}'_2$ *with*

$$\mathbf{r}_1 = (x_1, y_1),\ \textit{etc}$$

and two midpoints $\overline{\mathbf{r}}_1$ *and* $\overline{\mathbf{r}}_2$*:*

$$\begin{aligned}\overline{x}_1 &= \tfrac{1}{2}(x_1 + x'_1)\\ \overline{y}_1 &= \tfrac{1}{2}(y_1 + y'_1).\end{aligned}$$

We then have

$$|\overline{\mathbf{r}}_1 - \overline{\mathbf{r}}_2|_\gamma \leq \frac{|\mathbf{r}_1 - \mathbf{r}_2|_\gamma + |\mathbf{r}'_1 - \mathbf{r}'_2|_\gamma}{2}.$$

We have $|\mathbf{r}_1 - \mathbf{r}_2|_\gamma = |\mathbf{r}'_1 - \mathbf{r}'_2|_\gamma = |\overline{\mathbf{r}}_1 - \overline{\mathbf{r}}_2|_\gamma$ *only for parallel transport:* $\mathbf{r}_1 = \mathbf{r}'_1 + \mathbf{c}; \mathbf{r}_2 = \mathbf{r}'_2 + \mathbf{c}$.

Proof. Follows from triangle inequality $|\mathbf{a} + \mathbf{b}| \leq |\mathbf{a}| + |\mathbf{b}|$, with $\mathbf{a} = \mathbf{r}_1 - \mathbf{r}_2$ and $\mathbf{b} = \mathbf{r}'_1 - \mathbf{r}'_2$ with equality only for parallel transport. □

Note that if $|\mathbf{r}_1 - \mathbf{r}_2| \neq |\mathbf{r}'_1 - \mathbf{r}'_2|$, the midpoint distance $|\overline{\mathbf{r}}_1 - \overline{\mathbf{r}}_2|$ is smaller than $\max_i |\mathbf{r}_i - \mathbf{r}'_i|$.

Proposition 4 (Unique stable representation in the plane). *Each graph G has a unique stable representation in the plane (up to parallel transport).*

Proof. We assume the contrary. Let representations $\mathcal{E}^0$ and $\mathcal{E}^1$, realized by vectors $\mathbf{r}_i^0$ and $\mathbf{r}_i^1$, be two stable representation. We can assume $\mathcal{E}^0 \leq \mathcal{E}^1$.

Consider the representations $\mathcal{E}^\alpha$ realized by

$$\mathbf{r}_i^\alpha = \mathbf{r}_i^0 + \alpha \times \left[\mathbf{r}_i^1 - \mathbf{r}_i^0\right] \quad 0 \leq \alpha \leq 1.$$

The representations $\mathcal{E}^\alpha$ exist. We denote by e^0 and e^1 the representations of edge e in $\mathcal{E}^0$ and $\mathcal{E}^1$, respectively. Let $e_1^1, \ldots, e_m^1$ be the ordered vector of edge lengths. Let k be the smallest index such that e_k^0 is not parallely transported to e_k^1. We observe the following: if e is an edge of G such that $l(e^1) = l(e_k^1)$, then $l(e^0) \leq l(e_k^1)$ since $\mathcal{E}^0 \leq \mathcal{E}^1$. It means by Lemma 11 that $\mathcal{E}^\alpha < \mathcal{E}^1\ \forall \alpha < 1$, which implies that $\mathcal{E}^1$ is not stable. □

Proposition 5 (Unique stable representation on torus). *Each graph G has a unique stable representation on the torus if the sets of edges crossing each boundary are prescribed (up to parallel transport).*

Proof. The representations $\mathcal{E}^\alpha$ of the previous proof can analogously be applied to the corresponding periodic representations, both for edges in the inside of one rectangle and for the edges going across the boundary. □

This means that the number of stable representations of a toroidal graph is bounded by the number of possible sets of boundary horizontal and vertical edges.

Next we will discuss uniqueness of stable embeddings on the hemisphere. The following Lemma 12 is a nontrivial variant of Lemma 11: Obviously, the triangle inequality remains valid in three dimensions, but the midpoint would not lie on the surface of the sphere.

Lemma 12. *Consider three-dimensional vectors* $\mathbf{r}_1, \mathbf{r}_2, \mathbf{r}'_1, \mathbf{r}'_2$ *on the unit hemisphere with*

$$\mathbf{r}_1 = (x_1, y_1, z_1 = +\sqrt{1 - x_1^2 - y_1^2}),\ \textit{etc.}$$

and two midpoints $\overline{\mathbf{r}}_1$ *and* $\overline{\mathbf{r}}_2$ *which are defined with respect to a projection of vectors on the equator* $z = 0$

$$\overline{x}_i = \tfrac{1}{2}(x_i + x'_i);\ \overline{y}_i = \tfrac{1}{2}(y_i + y'_i);\ \overline{z}_i = \sqrt{1 - \overline{x}_i^2 - \overline{y}_i^2} \quad i = 1, 2. \tag{3}$$

We then have, for the three-dimensional Euclidean distance-squared:

$$|\overline{\mathbf{r}}_1 - \overline{\mathbf{r}}_2|^2 \le \frac{|\mathbf{r}_1 - \mathbf{r}_2|^2 + |\mathbf{r}'_1 - \mathbf{r}'_2|^2}{2}. \tag{4}$$

In (4), we can have equality only for generalized parallel transport with $x_1 - x'_1 = c(x_2 - x'_2)$ *and* $y_1 - y'_1 = c(y_2 - y'_2)$ *for special values of* c.

Proof. We can write (4) as

$$(\overline{z}_1 - \overline{z}_2)^2 \le -\left[\frac{x_1 + x'_1}{2} - \frac{x_2 + x'_2}{2}\right]^2 + \frac{(x_1 - x_2)^2}{2} + \frac{(x'_1 - x'_2)^2}{2}$$
$$+ \text{same terms in } y, y' + \tfrac{1}{2}(z_1 - z_2)^2 + \tfrac{1}{2}(z'_1 - z'_2)^2. \tag{5}$$

Explicit calculation shows that the terms on the first row of expression (5) is

$$-\left[\frac{x_1 + x'_1}{2} - \frac{x_2 + x'_2}{2}\right]^2 + \frac{(x_1 - x_2)^2}{2} + \frac{(x'_1 - x'_2)^2}{2}$$
$$= \tfrac{1}{4}[x_1 - x_2 - x'_1 + x'_2]^2,$$

which allows to show that (5) and (4) are equivalent to

$$(\overline{z}_1 - \overline{z}_2)^2 \le \tfrac{1}{4}\left(x_1 - x_2 - x'_1 + x'_2\right)^2 + \tfrac{1}{4}\left(y_1 - y_2 - y'_1 + y'_2\right)^2$$
$$+ \tfrac{1}{2}\left(z_1 - z_2\right)^2 + \tfrac{1}{2}\left(z'_1 - z'_2\right)^2. \tag{6}$$

Furthermore, we have, from eq. (3)

$$\overline{z}_i^2 = 1 - \left(\frac{x_i + x'_i}{2}\right)^2 - \left(\frac{y_i + y'_i}{2}\right)^2$$
$$= \tfrac{1}{4}(x_i - x'_i)^2 + \tfrac{1}{4}(y_i - y'_i)^2 + \tfrac{1}{2}(z_i^2 + z_i'^2) \quad i = 1, 2.$$

The inequality (6) now follows from the triangle inequality $(|\mathbf{a}| - |\mathbf{b}|)^2 \leq |\mathbf{a} - \mathbf{b}|^2$ with the four-dimensional vectors

$$\mathbf{a} = \left(\frac{z_1}{\sqrt{2}}, \frac{z_1'}{\sqrt{2}}, \frac{x_1 - x_1'}{2}, \frac{y_1 - y_1'}{2} \right)$$
$$\mathbf{b} = \left(\frac{z_2}{\sqrt{2}}, \frac{z_2'}{\sqrt{2}}, \frac{x_2 - x_2'}{2}, \frac{y_2 - y_2'}{2} \right),$$

which evidently satisfy $|\mathbf{a}| = \overline{z}_1$, $|\mathbf{b}| = \overline{z}_2$ and $|\mathbf{a} - \mathbf{b}|^2$ equal to the r.h.s. of (6). □

Proposition 6 (Unique stable rep. on hemisphere). *Each graph G on the hemisphere with fixed outer vertices has a unique stable representation.*

Proof. Using the definition of midpoints on the sphere from Lemma 12, we can define valid representations $\mathcal{E}^\alpha$ as in the proof of Proposition 4. Then we still have $\mathcal{E}^\alpha < \mathcal{E}^1 \ \forall \alpha < 1$. It is easy to see that, with fixed outer vertices, generalized parallel transport is impossible. □

2.3 Stable representations on the sphere

On the sphere, there can be several non-trivial stable representations. To see this, consider the equator-representation of Fig. 7. Besides a central cycle, at $z = 0$, there are vertices in the

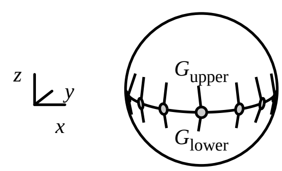

Figure 7: An equator embedding of a graph G, with a central cycle at $z = 0$, and upper and lower subgraphs G_{upper} (at $z > 0$) and G_{lower} (at $z < 0$). The edges on the central cycle are longer than all other edges.

upper subgraph G_{upper} (with $z > 0$) and in the lower subgraph G_{lower} (at $z < 0$). Furthermore, we suppose that the edges on the central cycle are longer than those in the rest of the graph. An equator representation can give rise to two inequivalent representations, namely by pulling the central cycle *up* to $z > 0$, or *down* to $z < 0$.

Proposition 6 allows us to observe that nevertheless, some degree of uniqueness can be preserved.

Proposition 7 (Unique representation with fixed cut). *There is unique stable representation of a graph on a sphere when the edges crossing a given equator are fixed.*

As mentioned in the introduction, extensive computing experiments suggest the stronger statement of Conjecture 2. This would imply that a given graph has only a finite number of stable representations (up to symmetry operations).

3 Jamming

In this section we derive basic properties of jammed configurations of disks on planar region, torus and sphere.

Definition 8 (Jammed embedding). *An embedding $\mathcal{E}$ of a graph is* jammed *if*

1. *$\mathcal{E}$ belongs to the convex hull of the set $\mathcal{O}$ of outer vertices, and each outer vertex is connected to at least one inner vertex.*
2. *$\mathcal{E}$ is* regular*, i.e. all edges have rescaled length d and the distance between any two vertices k, l not connected by an edge is strictly bigger than d.*
3. *there is a δ such that no representation $\mathcal{E}'$ with $|\mathbf{r}'_i - \mathbf{r}_i| < \delta$ has some edge longer and no edge shorter than in $\mathcal{E}$.*

The three central disks in Fig. 8 are not jammed, even though each one cannot move individually.

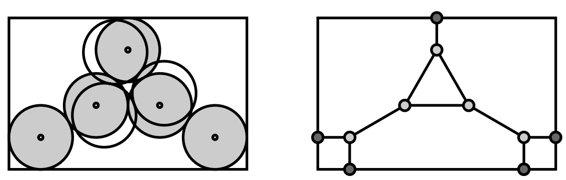

Figure 8: *Left:* Configuration of five disks, in which no disk can move by itself, but three disks can move together, as indicated. *Right:* The (unjammed yet stable) embedding corresponding to the configuration. The edges among outer vertices are omitted.

Let us recall that in a representation, the set $\mathcal{O}$ of outer vertices forms a subdivision of a convex n–gon. Let us denote this cycle of outer vertices by $C_{\mathcal{O}}$ and if G is a jammed embedding then let us denote by $G_{\mathcal{O}}$ the pseudo–embedding obtained from G by adding the edges of $C_{\mathcal{O}}$; let us note that $C_{\mathcal{O}}$ bounds the outer face of $G_{\mathcal{O}}$. In a jammed embedding G each inner vertex has degree bigger than two and at most five on the sphere, and at most six on planar region and torus. If $G_{\mathcal{O}}$ is two-connected then each inner face is convex ([7]). Below we show that each jammed graph $G_{\mathcal{O}}$ is three-connected.

Lemma 13. *If a graph G is connected but not two-connected and has no vertex of degree 1, then there are two vertices v_1, v_2 (possibly $v_1 = v_2$) and components G_i of $G \setminus v_i$ ($i = 1, 2$) such that each $G_i \cup v_i$ is two-connected and $G_1 \cup v_1$ is a subgraph of $G \setminus G_2$.*

Lemma 14. *If a graph G is two-connected but not three-connected, and has no vertex of degree 2, then it has two pairs V_1, V_2 of vertices (possibly with $V_1 \cap V_2 \neq \emptyset$) and components G_i of $G \setminus V_i$ ($i = 1, 2$) such that $G_i \cup V_i$ is two-connected and $G_1 \cup V_1$ is a subgraph of $G \setminus G_2$.*

Definition 9. *Let G be a two-connected regularly embedded graph, let F be a face of G bounded by a cycle C and let $v \in C$. We say that v is convex with respect to F if there is a plane containing v and perpendicular to the surface (planar region, torus, sphere), so that a small neighborhood of v in F lies completely in one half-space defined by the plane.*

We note that if F is a convex region bounded by a cycle then each vertex of the cycle is convex with respect to F.

Lemma 15. *Let F_1, F_2 be connected regions bounded by cycles C_1, C_2 and such that none of them covers the whole planar region (torus, sphere, hemisphere), but $F_1 \cup F_2$ do. Then there are at least three non-convex vertices of C_1 with respect to F_1 or of C_2 with respect to F_2.*

Proof. Cycle C_2 must be embedded inside F_1 and F_2 must be the region defined by C_2 that is not a subset of F_1. Then C_2 is a non-self-intersecting cycle on F_1. As such, it must have at least three sharp corners on F_1. □

Proposition 8 (Jammed graph three-connected). *If an embedding G is jammed, then $G_{\mathcal{O}}$ is three-connected.*

Proof. Let $G_{\mathcal{O}}$ be a minimum counter-example. If $G_{\mathcal{O}}$ is not connected then each component is jammed and three-connected by the minimality assumption. Consider the embeddings of different components G_1 and G_2 in the embedding of G. G_1 is completely embedded in one of the faces of G_2 and vice versa, which is not possible by convexity of faces and by Lemma 15.

If $G_{\mathcal{O}}$ has a vertex of degree at most two then it cannot be jammed. Therefore, we suppose that $G_{\mathcal{O}}$ is without a vertex of degree two and either connected or two-connected. By Lemma 13 and Lemma 14 there is a subset of vertices V_1 and a component G_1 of $G_{\mathcal{O}} \setminus V_1$ such that $G_1 \cup V_1$ is two-connected and has one of the following two properties:
1.V_1 consists of a single vertex v_1 and there is a vertex v_2 with $V_2 = \{v_2\}$ and a component G_2 of $G_{\mathcal{O}} \setminus V_2$ so that $G_2 \cup V_2$ is a two-connected subgraph of $G_{\mathcal{O}} \setminus G_1$.
2. V_1 consists of two vertices and there is a subset V_2 of *two* vertices and a component G_2 of $G_{\mathcal{O}} \setminus V_2$ so that $G_2 \cup V_2$ is a two-connected subgraph of $G_{\mathcal{O}} \setminus G_1$.

We consider the embedding of $G_1 \cup V_1$ induced by the embedding of $G_{\mathcal{O}}$ (see Fig. 9). Let F_1 be the face in which $G_{\mathcal{O}} \setminus G_1$ is embedded and let C_1 be the bounding cycle of F_1. Clearly $V_1 \subset C_1$. Moreover F_1 cannot be the outer face of the embedding of $G_{\mathcal{O}}$ since $G_{\mathcal{O}} \setminus G_1$ is embedded there. Hence all the vertices of $C_1 \setminus V_1$ are convex with respect to F_1.

Let F_2 be the face of the induced embedding of $G_2 \cup V_2$ which contains C_1 and let C_2 be the cycle that bounds F_2. Clearly $V_2 \subset C_2$ and as above, F_2 cannot be the outer face of the embedding of $G_{\mathcal{O}}$. Hence all vertices of $C_2 \setminus V_2$ are convex with respect to F_2. Then F_1, F_2, C_1, C_2 satisfy the properties of Lemma 15 but V_1 and V_2 have only two vertices, a contradiction. □

Proposition 9 (Jammed graphs stable). *Jammed embeddings are stable on the planar region and torus and on a hemisphere. On the sphere, jammed embeddings are stable if we fix representations of edges across an equator.*

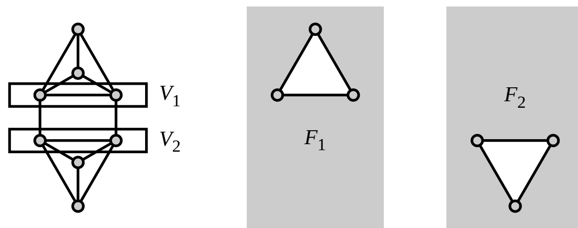

Figure 9: Faces F_1 and F_2, and subsets of vertices V_1 and V_2 used in the proof of Proposition 8.

Proof. We show that an unstable regular embedding $\mathcal{E}$ has a small move which leaves some edges the same and increases the others, which means that it is not jammed. For any $\delta > 0$, there is a representation $\mathcal{E}'$ within δ of $\mathcal{E}$ such that some edges decrease in length, and the others stay the same. Let $\mathcal{E}''$ be the inverse of the move which took $\mathcal{E}$ into $\mathcal{E}'$ (on the hemisphere: inverse of the projected move). The inverse move exists, since a jammed embedding in the plane or on the torus cannot have an outer vertex on an end point of the corresponding line segment, and for the hemisphere, if originally an inner vertex positioned on the equator moved, then $\mathcal{E}$ could not have been jammed. For the representation e of an edge in $\mathcal{E}$, let e' and e'' be the respective representations of the same edge in $\mathcal{E}'$ and $\mathcal{E}''$. We can use Lemma 11 (on planar region and torus) and Lemma 12 (for the hemisphere) to show that $l(e') = l(e) \implies l(e'') \geq l(e)$ and $l(e') < l(e) \implies l(e'') > l(e)$. □

The converse of Proposition 9 is not true, and stable representations are not necessarily jammed. An example is shown in Fig. 8.

As mentioned in the introduction, extensive computing experiments suggest, for the sphere, the stronger statement of Conjecture 2.

4 Algorithms

In Section 2.1, we discussed a finite algorithm for the determination of the $\mathcal{M}$–center of vectors $\mathbf{r}_i$. This algorithm is of practical use because a circle in d–dimensional space is already specified by $d+1$ points. The incremental *minover* algorithm [8] remains useful in high dimension d and is trivial to implement. For a finite number of vectors $\mathbf{r}_i, i \in I$ on the unit sphere, it is defined by

$$\mathbf{R}_0 = 0, \quad \mathbf{R}_{k+1} \leftarrow \mathbf{R}_k + \mathbf{r}_{i_{\min}},$$

where the index $i_{\min}$ is a minimal overlap (scalar product) vector with

$$\langle \mathbf{R}_k, \mathbf{r}_{i_{\min}} \rangle = \min_{i \in I} \langle \mathbf{R}_k, \mathbf{r}_i \rangle.$$

It can be proven [8] that

$$\mathbf{R}_k / |\mathbf{R}_k| \to \mathbf{r}_\infty$$

under the condition that a vector $\mathbf{R}$ exists with $\langle \mathbf{R}, \mathbf{r}_i \rangle > 0 \; \forall i \in I$.

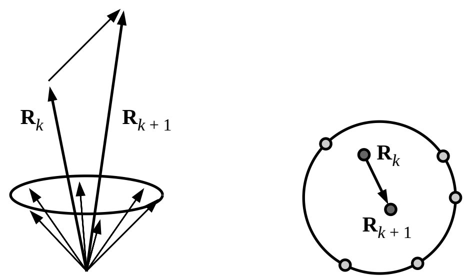

Figure 10: *Left:* Minimum overlap algorithm. The rescaled vector $\mathbf{R}_k/|\mathbf{R}_k|$ converges to the $\mathcal{M}$–center of vectors on the sphere. *Right:* On the plane, the move is in direction of the vector $\mathbf{r}_i$ with maximum distance to $\mathbf{R}_k$. The amplitude ϵ_k of the move decreases with k, but $\sum_k \epsilon_k$ diverges.

In the minover algorithm (on the sphere), the corrections to $\mathbf{R}_k$ decrease with increasing k. On the plane or the torus, we can do the same by using an update

$$\mathbf{R}_{k+1} \leftarrow \mathbf{R}_k + \epsilon_k \left[\mathbf{r}_{i_{\max}} - \mathbf{R}_k\right],$$

where $\mathbf{r}_{i_{\max}}$ is the vector of maximum distance to $\mathbf{R}_k$ (see Fig. 10), and where the sequence ϵ_k satisfies the conditions:

$$\epsilon_k \rightarrow 0 \text{ for } k \rightarrow \infty$$
$$\sum_k \epsilon_k \rightarrow \infty \text{ for } k \rightarrow \infty.$$

This algorithm was applied to all vertices sequentially in order to compute stable $\mathcal{M}$–repre-sen-ta-tions.

As a simple test, we have run this algorithm on the three-connected graph of Fig. 1 and Fig. 3, embedded on a sphere and starting from an equator position. This graph, incidentally, corresponds to the conjectured optimal packing for the thirteen-sphere problem. The algorithm converges rapidly to the conjectured optimum solution [6], which is shown in Fig. 11.

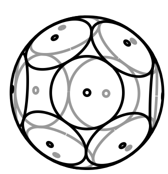

Figure 11: Conjectured optimal configuration of 13 disks on a unit sphere, and corresponding representation of vertices, obtained by computational experiment as stable $\mathcal{M}$–representation of the graph of Fig. 1 and Fig. 3. The algorithm of Section 4 was used.

As stated in Conjecture 1, we are convinced that a finite algorithm for computing a stable $\mathcal{M}$–representation exists.

Acknowledgment. We are indebted to F. Bouchut for the proof of Lemma 12 and to J. Mlcek for discussion on lexicographic order and energy. This work has been supported by the European Science Foundation (ESF) program "Phase Transitions and Fluctuation Phenomena for Random Dynamics in Spatially Extended Systems". We thank ITI Prague and LPS-ENS for hospitality.

References

[1] W. T. Tutte, *How to draw a graph.* Proc. London Math. Soc. **13**, 743-768 (1963).

[2] M. D. Rintoul, S. Torquato, *Metastability and Crystallization in Hard-Sphere Systems.* Phys. Rev. Lett. **77**, 4198-4201 (1996).

[3] L. Santen, W. Krauth, *Absence of thermodynamic phase transition in a model glass former.* Nature **405**, 550-551 (2000).

[4] W. Krauth, *Disks on a Sphere and Two-Dimensional Glasses.* Markov Processes Relat. Fields **8**, 215-219 (2002).

[5] J. H. Conway, N. J. A. Sloane, *Sphere Packings, Lattices and Groups* (Springer, New York, 1993).

[6] D. A. Kottwitz, *The Densest Packing of Equal Circles on a Sphere.* Acta Cryst. **A47**, 158-165 (1991).

[7] K. Schütte, B. L. van der Waerden, *Auf welcher Kugel haben 5,6,7,8 oder 9 Punkte mit Mindestabstand Eins Platz.* Math. Ann. **123**, 223-234 (1951),

Das Problem der dreizehn Kugeln. Math. Ann. **125**, 325-334 (1953).

[8] W. Krauth, M. Mézard, *Learning algorithms with optimal stability in neural networks.* J. Phys. A: Math Gen. **20**, L745-L752 (1987).

[9] M. Berger "La treizième sphère" *Dossier 'Pour la Science' October/December 2003*, 68-71.

[10] R. M. Robinson, *Arrangement of 24 points on a sphere.* Math. Ann. **144**, 17-48 (1961).